Chemosphere 291 (2022) 132939

Contents lists available at ScienceDirect

Chemosphere

journal homepage: www.elsevier.com/locate/chemosphere

Enzymatic synthesis and formation kinetics of mono- and di-hydroxylated chlorinated paraffins with the bacterial dehalogenase LinB from *Sphingobium indicum*

Marco C. Knobloch [a,b,*], Flurin Mathis [a,c], Thomas Fleischmann [d], Hans-Peter E. Kohler [d], Susanne Kern [c], Davide Bleiner [a,b], Norbert V. Heeb [a]

[a] Laboratory for Advanced Analytical Technologies, Swiss Federal Institute for Materials Science and Technology Empa, Überlandstrasse 129, 8600, Dübendorf, Switzerland
[b] Department of Chemistry, University of Zürich, Winterthurerstrasse 190, 8057, Zürich, Switzerland
[c] Zürich University of Applied Sciences ZHAW, Einsiedlerstrasse 31, 8820, Wädenswil, Switzerland
[d] Swiss Federal Institute of Aquatic Research and Technology Eawag, Überlandstrasse 129, 8600, Dübendorf, Switzerland

HIGHLIGHTS

- Enzymatic synthesis of mono- and di-hydroxylated chloroparaffins.
- 15 mono- and 15 di-hydroxy-CP homologues were studied by LC-MS.
- Deconvolution of interfered hydroxylated CP-, CO- and CdiO-mass spectra.
- Preferential formation of lower-chlorinated SCCP-ols and SCCP-diols by LinB.
- Homologue-specific kinetic models describe stepwise dehalohydroxylation.

GRAPHICAL ABSTRACT

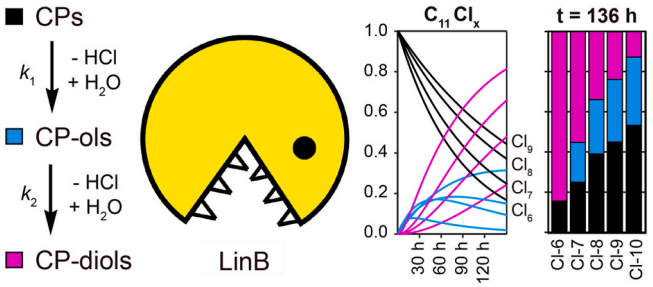

ARTICLE INFO

Handling Editor: Derek Muir

Keywords:
Enzymatic dehalohydroxylation
Hydroxylated chloroparaffins (CP-ols)
Dihydroxylated chloroparaffins (CP-diols)
In-vitro CP transformation
Persistent organic pollutants (POPs)

ABSTRACT

Transformation studies of chlorinated paraffins (CPs) and the effects of CP transformation products on humans, biota and environment are rare. The focus here is on hydroxylation reactions. As for polyhalogenated persistent organic pollutants (POPs) in general, hydroxylation reactions convert lipophilic material to more polar compounds with increased mobility. We investigated the *in-vitro* transformation of single-chain CP-mixtures to hydroxylated products with the dehalogenase LinB from *Sphingobium indicum*. C_{11}-, C_{12}- and C_{13}-single-chain CP-homologues were exposed to LinB and mono-hydroxylated (CP-ols) and di-hydroxylated (CP-diols) transformation products were formed. Liquid-chromatography coupled to mass-spectrometry (LC-MS) was used to detect hydroxylated products and to separate them from the starting material. The presented data can be used to identify these CP-ol and CP-diol homologues in other samples. Hydroxylated products had lower chlorination degrees (n_{Cl}) than respective CP-starting-materials. Reactive and persistent CP-material was found in each homologue group. Reactive material is converted within hours by LinB, while more persistent CPs are transformed within days. Homologue-specific kinetic models were established to simulate the stepwise hydroxylation of persistent CPs to mono- and di-hydroxylated products. First-order rate constants for the formation of CP-ols (k_1)

* Corresponding author. Laboratory for Advanced Analytical Technologies, Swiss Federal Institute for Materials Science and Technology Empa, Überlandstrasse 129, 8600, Dübendorf, Switzerland.
E-mail address: marco.knobloch@empa.ch (M.C. Knobloch).

https://doi.org/10.1016/j.chemosphere.2021.132939
Received 27 June 2021; Received in revised form 11 November 2021; Accepted 14 November 2021
Available online 18 November 2021

and CP-diols (k_2) were deduced for different homologues. Lower-chlorinated CP-ols did not accumulate to large extent and were transformed quickly to CP-diols, while higher-chlorinated CP-ols and -diols both accumulated. By enzymatic transformation of single-chain CPs with LinB, we synthesized unique sets of mono- and di-hydroxylated materials, which can be used as analytical standards and as starting materials for metabolic, toxicity and environmental fate studies.

1. Introduction

Chlorinated paraffins (CPs) are widely used as plastic additives e.g. as plasticizers and flame retardants (Fiedler, 2010; UNEP, 2016). They are also used as non-flammable liquids and coolants in the metal working industry (Fiedler, 2010; UNEP, 2016). CPs are high production volume chemicals produced at rates above the million tons per year (Glüge et al., 2016; van Mourik et al., 2016). In 2017, short-chain CPs (SCCPs, C_{10}–C_{13}) have been included to the Stockholm Convention on persistent organic pollutants (POPs) (UNEP, 2017a). Hence, the global CP production shifted towards medium- and long-chain CPs to fullfil the market needs (Schinkel et al., 2018a).

As CPs are released into the environment, it is inevitable that they are also exposed to water. A stepwise hydrolysis of CPs can lead to mixed hydroxylated and chlorinated products (Knobloch et al., 2021a). In other words, CPs can be hydroxylated in steps to mono- and subsequently to di-hydroxylated transformation products. These transformation products are more polar with increased water solubility. To the best of our knowledge, hydroxylated CPs were not reported in the environment, but they are identified as metabolites (Chen et al., 2020; He et al., 2020). Reference materials for mono- and di-hydroxylated CPs are not available which complicates their analysis. In this study, we propose an enzyme-catalyzed process to produce mono- and di-hydroxylated CPs.

Fig. 1 highlights some of the expected CP transformation reactions, all of them leading to dechlorinated and oxygenated products (Vogel et al., 1987; Belkin, 1992; Faber, 2018). The reactions shown are set in context to CPs in the following.

Reductive dehalogenation transforms CPs to lower-chlorinated CPs (Fig. 1A) (Li et al., 2019; Chen et al., 2020). In case of technical CP-mixtures, which contain several Cl-homologues, such transformations lead to similar CP-mixtures with lower chlorination degrees.

The loss of hydrochloric acid (HCl) transforms paraffinic to olefinic material (Fig. 1B) with one double bond equivalent (DBE). This has been observed during the exposure of CPs to heat (>150 °C) and reactive metal surfaces (Schinkel et al., 2018b, 2018c, 2018c). It could also be shown that the bacterial dehydrohalogenase LinA2 from *Sphingobium indicum* catalyzes a step-wise elimination of HCl converting CPs to COs and CdiOs as shown in Fig. 1B (Heeb et al., 2019).

Hydroxylations of CPs (Fig. 1C,E) lead to chloroparaffinols (CP-ols). Such reactions can occur under abiotic and biotic conditions as discussed herein. A nucleophilic substitution of chlorine with a hydroxyl group leads to CP-ols with lower chlorination degrees (Fig. 1C). An exchange of hydrogen with a hydroxyl group leads to CP-ols too, but does not affect the chlorination degree (Fig. 1E).

Hydroxylation reactions eventually also produce halohydrins. From a chemical and toxicological point of view, halohydrins can be considered as reactive intermediates that can undergo further transformations *in-vitro* and *in-vivo* to produce e.g. epoxides (Fig. 1D) and carbonyls (Fig. 1F). Both classes of compounds have one DBE and interfere with

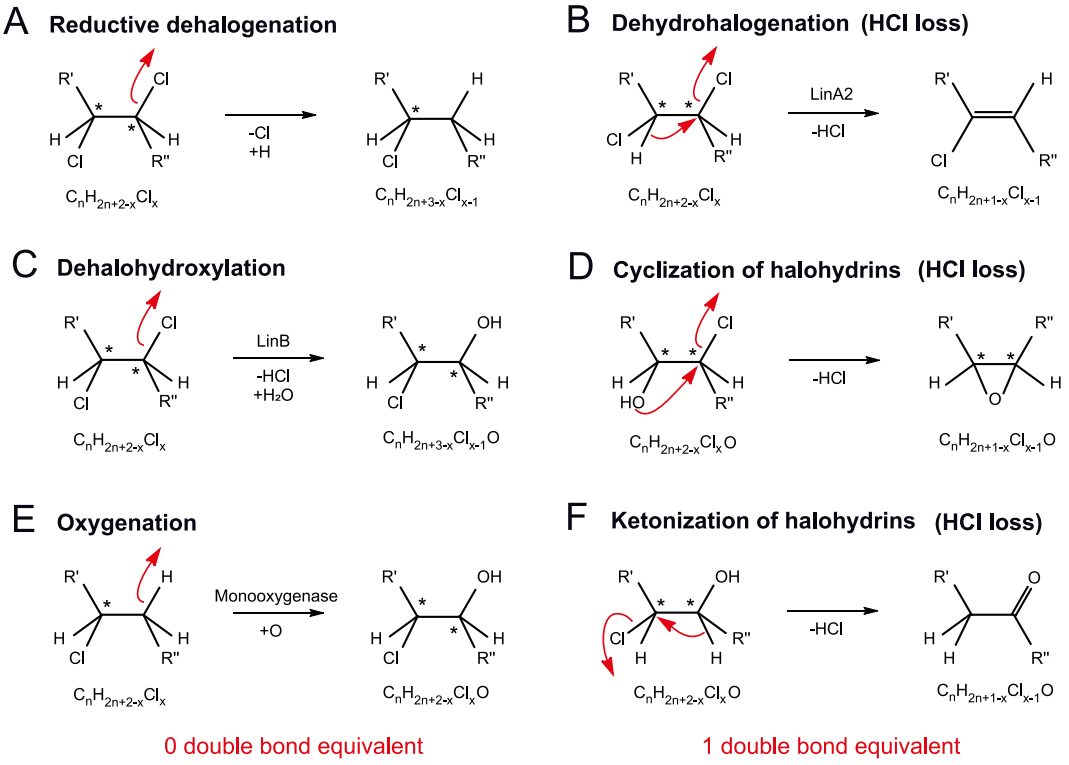

Fig. 1. Abiotic and enzyme-catalyzed transformation reactions of CPs. Reductive dechlorination (A) and dehydrohalogenation (B) reactions lead to paraffinic (0 double bond equivalent, DBE) and olefinic (1 DBE) materials with lower chlorination degrees. Substitution reactions of chlorine (C) and hydrogen (E) by hydroxyl groups lead to hydroxylated CPs (CP-ols). In certain cases, halohydrins (-CX–COH–) will form via hydroxylation reactions. Such halohydrins can undergo elimination reactions of HCl to form epoxides (D) and carbonyl compounds (F) with 1 DBE.

mass spectra of chloroolefin-ols (Knobloch et al., 2021a). Things further complicate if multiple dehalogenation and oxygenation reactions occur, which in general has to be expected for polyhalogenated compounds.

The analysis of CP transformation products with variable chlorination degrees, DBEs and carbon chain lengths is challenging. Severe mass spectrometric interferences of paraffinic (0 DBE) and olefinic (>0 DBE) materials have to be expected (Schinkel et al., 2017, 2018c; Heeb et al., 2019). CP mass spectra can be interfered with those of chloroolefins (COs, 1 DBE) and chlorodiolefins (CdiO, 2 DBE), which are only resolved at mass resolutions >27′000 (Knobloch et al., 2021a). Accordingly, also hydroxylated transformation products can contain unsaturated materials. Mass spectra of saturated hydroxylated CPs (0 DBE) and unsaturated hydroxylated COs, ethers, epoxides and carbonyls (>0 DBE) are interfered as well (Fig. 1). To resolve such interferences, a mass resolution >68′000 is needed. If not available, a mathematical deconvolution procedure can be applied (Schinkel et al., 2017, 2018c; Knobloch et al., 2021a). We showed that liquid chromatography coupled to atmospheric pressure chemical ionization and a quadrupole time-of-flight mass detector (LC-APCI-QToF-MS) can be used to analyze mixtures of CPs and hydroxylated transformation products (Knobloch et al., 2021a, 2021b, 2021b). Hydroxylated materials were separated from non-hydroxylated ones by LC and interferences of saturated and unsaturated materials were resolved using the mentioned mathematical deconvolution method (Knobloch et al., 2021a, 2021b).

Only few examples of enzymatic CP transformations are known. We showed that the bacterial dehydrohalogenase LinA2 from *Sphingobium indicum* catalyzes a step-wise elimination of HCl converting CPs to chloro-olefins (COs) and –diolefins (CdiOs) as shown in Fig. 1B (Heeb et al., 2019).

We have also shown that the dehalogenase LinB from *Sphingobium indicum* transforms CPs (Knobloch et al., 2021a, 2021b). CP-ols were formed as first-generation and CP-diols as second-generation products. The mechanism of LinB-catalyzed dehalogenation reactions has been studied before for hexachlorocyclohexanes (HCHs) (Raina et al., 2007; Lal et al., 2010) and hexabromocyclododecanes (HBCDs) (Heeb et al., 2012, 2018). Fig. S1 displays the stepwise transformation of halides (-CHX-) as found in HCHs and HBCDs into respective alkyl-enzyme esters of aspartate-108 (Raina et al., 2007; Heeb et al., 2013). The Asp-108 carboxylate residue acts as the nucleophile replacing the halide (Raina et al., 2007; Heeb et al., 2013). Hydrolysis of the formed alkyl-enzyme ester leads to an alcohol and Asp-108. The transformation of HCHs and HBCDs is regio- and stereo-selective (Raina et al., 2008; Heeb et al., 2013).

In previous works, we emphasized the LinB-catalyzed transformation of CPs and COs towards hydroxylated transformation products (Knobloch et al., 2021a, 2021b). Here we used LinB to produce sets of C_{11}-, C_{12}- and C_{13}-CP-ols and -diols from respective single-chain CP-materials. These new hydroxylated materials can be used as analytical standards for metabolomic, toxicological and environmental fate studies. The provided LC-MS data can be used to identify CP-ols and CP-diols. Homologue-specific kinetic models for the formation of CP-ols and CP-diols were developed. These models included first-order rate constants which were deduced from time-dependent data, describing the step-wise formation of CP-ols and CP–diols and the accumulation of mono- and di-hydroxylated CPs with time.

2. Experimental

2.1. Substrates, enzyme expression and incubation

The procedure to obtain the enzyme LinB is described elsewhere (Heeb et al., 2012; Knobloch et al., 2021a). The *in-vitro* exposure of single-chain CP-materials has been described before and is just briefly described herein (Knobloch et al., 2021a, 2021b). Chloroundecanes (m_{Cl} = 65.25%), chlorododecanes (m_{Cl} = 65.08%) and chlorotridecanes (m_{Cl} = 65.18%, all from Dr. Ehrenstorfer, Augsburg, Germany) were used as substrates in separate experiments. Each single-chain CP-mixture (8 μg) was exposed to heterologously expressed LinB (400 μg, 0.0125 μmol, M_{LinB} = 32′000 kDa (Nagata et al., 1993)) in 4 mL aqueous buffer (pH 8.3) containing acetone (10 vol%), glycine (182 mM) and tris (hydroxymethyl)amino methane (25 mM). Aliquots (500 μL) were taken after 2, 4, 8, 24, 48, 72 and 144 h. Control samples exposed to buffer only were taken at start and after 144 h. Directly after taking samples, 500 μL ethyl acetate and internal standard (IS, γ-HBCD, 50 ng) were added and samples were stored at −20 °C. Aqueous phases were extracted with ethyl acetate (3 × 500 μL). The combined organic extracts were reduced to dryness by a nitrogen stream. The residues were dissolved in 100 μL methanol. Samples were analyzed (double injection, n = 2) by LC-APCI-QTOF-MS. Later discussed data refers to the mean of both measurements and standard deviations are indicated.

2.2. Chemical analysis using LC-APCI-QTOF-MS

The LC-APCI-QTOF-MS method applied was introduced before (Knobloch et al., 2021a) and is briefly described herein. A reversed-phase (RP) C_{18}-chromatographic column (Agilent, SB-C18 RRHD, 50 mm × 3 mm, 1.8 μm, 50 °C) was used with water and a mixture of methanol/dichloromethane (9/1) as eluents to separate mono- and di-hydroxylated CP-transformation products from CP-starting materials. Hydroxylated transformation products are more polar than CPs and eluted earlier from the column (Knobloch et al., 2021a). The infusion of dichloromethane results in the enhanced formation of chloride-adducts $[M+Cl]^-$ of CPs, CP-ols and CP-diols in the APCI module. The used Agilent 6520 QTOF-MS provides a mass resolution of ≈ 8′000 at the expected mass range of SCCPs and their hydroxylated metabolites. Various C_{11}-, C_{12}- and C_{13}-CP-ols and -CP-diols were identified according to the expected isotope clusters of their chloride-adducts without fragmentation (Tables S1-S18). The LC- and MS-system were not electronically synchronized. In order to provide reliable retention times, we calculated relative retention times (rrt) in relation to γ-HBCD (IS) which are listed in Tables S19 and S20.

2.3. Mathematical deconvolution of interfered mass spectra

CPs and CP-diols/CO-diols are separated with the chromatographic separation method described herein. However, paraffinic and olefinic materials with the same hydroxylation degree cannot be separated chromatographically. Therefore, a mathematical deconvolution method was used to resolve interfered mass spectra of paraffinic and olefinic materials (Fig. S2). The method has been described and improved before (Bogdal et al., 2015; Schinkel et al., 2017; Heeb et al., 2020; Knobloch et al., 2021a, 2021b). Interfered paraffin and olefin isotope clusters are recreated by a linear combination of calculated isotope clusters. With this procedure, paraffinic (p_{CP}), mono-olefinc (p_{CO}) and di-olefinic (p_{CdiO}) proportions of interfered isotope clusters of CPs/COs/CdiOs, CP-ols/CO-ols/CdiO-ols and CP-diols/CO-diols/CdiO-diols were obtained. Non-interfered and abundance-corrected signal intensities $I_{100\%}$ (mean, n = 2) were also obtained after mathematical deconvolution. These data are used to calculate homologue patterns and chlorination degrees based on the mass spectrometric abundance (Knobloch et al., 2021a, 2021b). In addition, kinetic rate constants of the formation of mono- and di-hydroxylated CP-transformation products were deduced.

2.4. Modeling of transformation kinetics

Bimodal first-order kinetic models were established to describe the transformation of persistent and reactive CP- and CO-homologues to hydroxylated transformation products (Knobloch et al., 2021b). With it, kinetic parameters of the CP conversion were obtained. Herein, we set up a second kinetic model to describe the formation of mono- and di-hydroxylated transformation products from CPs in the second slower phase. The model is based on the uni-directional, stepwise

dehalohydroxylation of CPs to first- (CP-ols) and second- (CP-diols) generation products as described later in detail (section 3.5). As input data, the kinetic parameters of the conversion of the starting material and the corrected, non-interfered $I_{100\%}$ signals of CPs, CP-ols and CP-diols were used. They are reported with standard deviations in Tables S21-S29. As described later, the products have a lower MS-response due to lower ionization efficiency relative to the starting material. Therefore, one has to expect some deviations because of the lower response, abundance and lower signal-to-noise ratios of the transformation products. Signals of CP-ols and CP-diols were corrected by a relative response factor. All measured data points were included in the model. Kinetic models for the formation of hydroxylated olefinic and diolefinic materials were not developed because of low abundances already in the starting material. Furthermore, no evidence was found that LinB catalyzes a formation of chloroolefins (Knobloch et al., 2021a). Kinetic parameters were deduced with Excel Solver (2016, Microsoft, Redmond USA). With these kinetic models, it is possible to estimate the time- and homologue-dependent proportions of CPs, CP-ols and CP-diols during LinB-exposure.

3. Results and discussion

3.1. Chromatographic characterization of hydroxylated CP transformation products

Fig. 2 displays, as example, extracted ion chromatograms (EICs) as sum of three characteristic chloride-adduct ions of mono- (A) and di-hydroxylated (B) products of C_{12}-CPs, exposed to LinB *in-vitro* for 144 h. Figure S3 also shows EICs of respective C_{11}- and C_{13}-CP-ols and -CP-diols. EICs of CP-ols and CP-diols show interferences from olefinic homologues because the LC-APCI-QTOF-MS used for measurements cannot resolve these signals as described in chapter 1, but mathematical deconvolution can (chapter 3.2). The reported EICs of CP-ols and CP-diols deliver valuable information such as retention times, which is useful to search for such compounds.

C_{12}-CPs (Fig. 2) and C_{13}-CPs (Fig. S3) were converted to respective Cl_6-, Cl_7-, Cl_8-, Cl_9- and Cl_{10}-CP-ols and further to Cl_5-, Cl_6-, Cl_7-, Cl_8- and Cl_9-CP-diols. C_{11}-CPs were converted to Cl_5- to Cl_{10}-CP-ols and Cl_4- to Cl_9-CP-diols (Fig. S3). In total, homologue groups of 15 CP-ols and 15 CP-diols are described by the shown EIC-data. In addition, Cl_3- and Cl_4-homologues of CP-ols and-CP-diols could be detected but are not shown due to low abundance, they are reported in section 3.2. Relative retention times of different homologues in relation to the internal standard (γ-HBCD) are listed in Tables S19 and S20 and indicated in Fig. 2 and Fig. S3. Relative retention times of CP-ols (A) increase gradually from 0.72 to 0.92 for Cl_6- to Cl_{10}-homologues. C_{12}-CP-diols show similar trends. Thus, lower-chlorinated C_{12}-CP-ols and -diols are more polar and eluted earlier from the reverse-phase column (C_{18}-RP) than higher-chlorinated ones. Similar trends are observed for C_{11}- and C_{13}-CP-ols and -diols (Fig. S3). In relation to the IS, the 15 CP-ols detected eluted in a range of 0.62–0.98, while the 15 CP-diols eluted from 0.20 to 0.54. Thus, mono- and dihydroxylated CPs can be separated under the given chromatographic conditions from respective starting materials. This facilitates the interpretation of mass spectra and allows a mathematical deconvolution of interfered spectra of paraffinic and olefinic material, as discussed later.

All CP-ols eluted as Gauss-like peaks from the C_{18}-RP column, while most CP-diols, eluted in two overlapping peaks (Fig. 2 and Fig. S3). Proportions of early-eluting CP-diols are higher than those of late-eluting diols. Respective ratios varied.

Thus, new mono- and di-hydroxylated CP-materials were produced by the *in-vitro* transformation of C_{11}-, C_{12}- and C_{13}-CPs with the enzyme LinB. Such materials are of interest as analytical standards to further investigate the formation of hydroxylated CPs in various metabolic and environmental processes. The given chromatographic library (Tables S19 and S20) can serve as a reference.

3.2. Mass spectra of hydroxylated CP transformation products

Mass spectra of chlorinated paraffins, olefins and respective hydroxylated transformation products overlap at mass resolution <20′000 (Knobloch et al., 2021a). To resolve interfered mass spectra, a mathematical deconvolution procedure shown in Fig. S2, was applied and paraffin- (p_{CP}), olefin- (p_{CO}) and diolefin- (p_{CdiO}) proportions were deduced. A chromatographic separation of non-, mono- and di-hydroxylated materials is a pre-requisite to apply the deconvolution procedure and to avoid additional interferences.

The stepwise dehalohydroxylation of C_{13}-CPs to respective CP-ols and CP-diols is already documented (Knobloch et al., 2021a). Fig. 3 displays mass spectra of C_{12}-CPols and –diols and Fig. S4 shows those of C_{11}- and C_{13}-CP-ols and –diols. Paraffinic and olefinic material cannot be separated chromatographically. Thus, the observed isotope clusters of

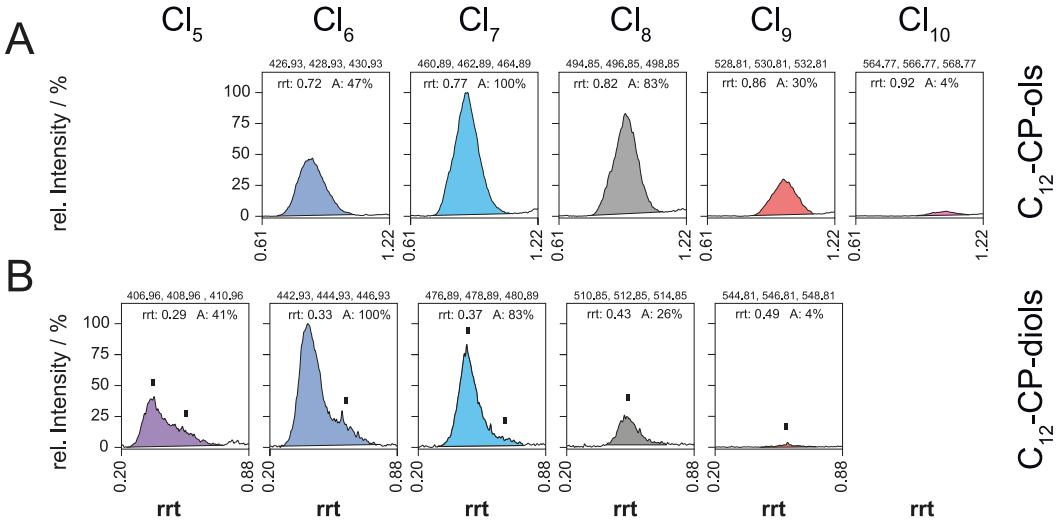

Fig. 2. Chromatographic description of mixed mono- and di-hydroxylated CPs. The sum of three characteristic ions of respective chloride-adducts $[M+Cl]^-$ without fragmentation are shown as EIC. Extracted *m/z* values are depicted above the corresponding chromatographic peak. Average retention times (rrt) relative to the internal standard (rac. γ-HBCD) are indicated. While mono-hydroxylated products (CP-ols) (A) elute as single Gauss-like peaks, two overlapping peaks are observed for most di-hydroxylated compounds (CP-diols) (B). Peaks are scaled to the mass spectrometric most abundant homologue (100%) in each class of compounds.

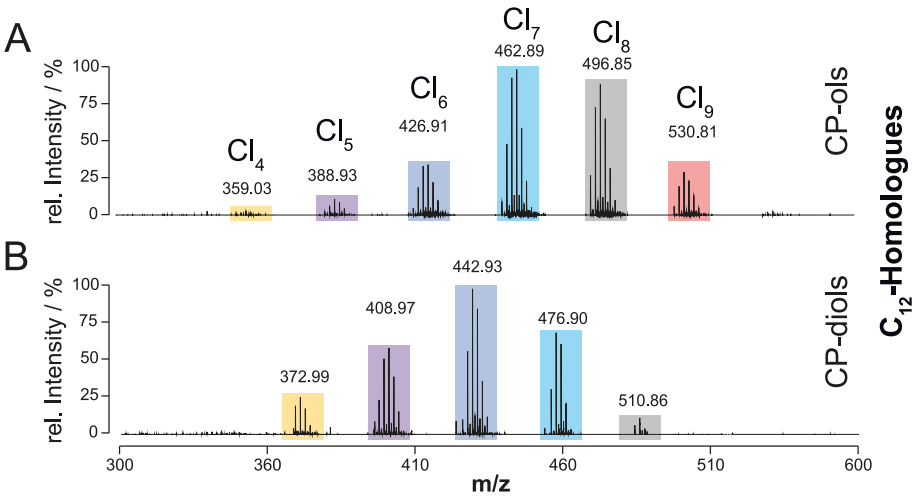

Fig. 3. Mass spectra (R~8000) of mono- and dihydroxylated C_{12}-CP transformation products. Exposure of a single-chain C_{12}-CP-material to the dehalogenase LinB for 144 h resulted in the formation of mono- (A) and di-hydroxylated (B) products. Chloride-adducts $[M+Cl]^-$ are formed under chloride-enhanced ionization conditions (CE-APCI). Isotopologues belonging to different homologue classes are highlighted and the most intense signals are indicated with the respective *m/z* value. Hepta-chlorinated compounds (Cl_7, light blue) are most abundant in CP-ol fraction, while hexa- (Cl_6, blue) chlorinated homologues dominate in CP-diol fractions. Tetra- (Cl_4, yellow), penta- (Cl_5, violet), octa- (Cl_8, gray) and nona- (Cl_9, red) chlorinated homologues were also detected. (For interpretation of the references to colour in this figure legend, the reader is referred to the Web version of this article.)

CP-ols (Fig. 3A and Fig. S4A,B) and CP-diols (Fig. 3B and Fig. S4C,D) show interferences with signals of olefinic and diolefinic material. Mass spectra with reduced chemical noise were obtained after background subtraction. The obtained isotope clusters are suitable for deconvolution.

The stepwise dechlorination (loss of HCl, *m/z*: -36, −38) and subsequent hydroxylation (addition of H_2O, *m/z*: +18) corresponds to net mass losses of *m/z*: -18, −20. Mass spectra of C_{12}-CP-ols (Fig. 3 A) and related CP-diols (Fig. 3 B) indeed differ by *m/z*: -18 and −20. Lower-chlorinated CP-diols (Fig. 3 B) are more abundant in the mass spectrum than respective CP-ols (Fig. 3 A). For example, Cl_7-homologues (light blue) are most abundant in the C_{12}-CP-ol spectrum (Fig. 3 A) while lower-chlorinated homologues such as Cl_5- (violet) and Cl_6-homologues (dark blue) dominate in the C_{12}-CP-diol spectrum (Fig. 3 B). Similar effects are observed for C_{11}- and C_{13}-homologues (Fig. S4).

3.3. Deconvolution of interfered mass spectra

Elimination of HCl converts paraffinic to olefinic material (Fig. 1D). Such elimination reactions can occur under abiotic conditions and under the influence of certain enzymes (Li et al., 2014; Schinkel et al., 2018b; Heeb et al., 2019). A hydroxyl group in vicinal position to a chloride also represents a potential reactive center (Faber, 2018). Such chlorohydrins may undergo HCl eliminations too to produce epoxides (Fig. 1D) and carbonyls (Fig. 1E). Like olefins, these compounds have one double bound equivalent (DBE). In other words, mass spectra of mono- and di-hydroxylated compounds (Fig. 3, S4) could show interferences with a variety of CP transformation products containing one or more DBEs (Knobloch et al., 2021a).

Therefore, we applied a mathematical deconvolution procedure (Fig. S2) and investigated isotope clusters in exposed and control samples of mono- and di-hydroxylated materials. The replicate analysis (n = 2) of mass spectra of four Cl-homologue clusters in three materials (C_{11}, C_{12}, C_{13}) for non-, mono- and di-hydroxylated compounds exposed for 0, 2, 4, 8, 24, 48, 72, 144 h and a control, resulted in extensive deconvolution work (648 homologue clusters).

Figs. S5 and S6 give examples for the deconvolution of isotope clusters of mono- and di-hydroxylated C_{11}-homologues. Tables S21 to S29 lists respective proportions of paraffinic (p_{CP}), olefinic- (p_{CO}), and diolefinic (p_{CdiO}) materials. In addition, non-interfered $I_{100\%}$ signal intensities (cts) were obtained with the deconvolution procedure (Fig. S2).

The deconvolution of mass spectra of mono- and di-hydroxylated products revealed that only small proportions of olefinic and diolefinic material can be found after 144 h. No indications for a LinB-catalyzed formation of additional olefinic material were found (Knobloch et al., 2021a, 2021b). In the following chapters, only non-interfered $I_{100\%}$ data (cts) of CPs, CP-ols and CP-diols obtained by mathematical deconvolution are processed (Tables S21 to S29.).

3.4. Changes of homologue pattern and chlorination degree during LinB-exposure

Homologue distributions and chlorination degrees of C_{12}-CPs and respective CP-ols and CP-diols are shown in Fig. 4. Respective data of C_{11}- and C_{13}-materials are shown in Figure S7. While nona- and octa-chlorinated homologues dominate in CP fractions, octa-, hepta- and hexa-CP-ols and hepta-, hexa- and penta-CP-diols are most abundant in the product fraction. Homologue distributions only change moderately during LinB-exposure and higher-chlorinated homologues become slightly more abundant with prolonged exposure time. These trends are also observed for C_{11}- and C_{13}-CPs, CP-ols and CP-diols. This indicates that lower-chlorinated homologues are more reactive towards LinB than higher-chlorinated ones and the later accumulate in the remaining material.

Fig. 4 and S7 also display chlorination degree (n_{Cl}) trends of CPs, CP-ols and CP-diols. Table S30 lists respective changes with standard deviations (n = 2). Chlorination degrees were deduced from non-interfered data as described in chapter 2.3. Moderate systematic changes of the chlorination degree of 0.1 up to 0.3 were observed during LinB-exposure. For example, n_{Cl} of C_{12}-CPs increased from 8.8 to 9.1 during exposure, those of CP-ols and CP-diols increased from 7.2 to 7.5 and from 6.1 to 6.2, respectively. Standard deviations for C_{12}-CPs and C_{12}-CP-ols were between 0.00 and 0.02, those of C_{12}-CP-diols with lower signal-to-noise-ratio were between 0.00 and 0.14. Similar effects can be observed for C_{11}- and C_{13}-homologues. The systematic increase of the chlorination degree for all observed homologues and appropriate standard deviations indicate that higher-chlorinated homologues accumulate during LinB-exposure. Nevertheless, chlorination degrees are lowered substantially with increasing hydroxylation degree by 1.4 to 1.9 from CPs to CP-ols and by 0.8 to 1.7 from CP-ols to CP-diols (Table S30). This corresponds to an overall decrease of the chlorination degree of 2.4 to 3.4 from CPs to CP-diols. These substantial reductions of chlorination degrees (n_{Cl}) indicates that LinB indeed catalyzed stepwise dehalohydroxylation reactions (Fig. 1C). Buffer-exposure did not induce a hydroxylation or changes of the homologue distribution of the starting materials (Knobloch et al., 2021b).

Furthermore, we noticed that lower-chlorinated precursors are converted faster by LinB than higher-chlorinated ones. This preference is also observed for mono- and di-hydroxylated substrates, resulting in an accumulation of higher-chlorinated material with time (Fig. 4 and Fig. S7).

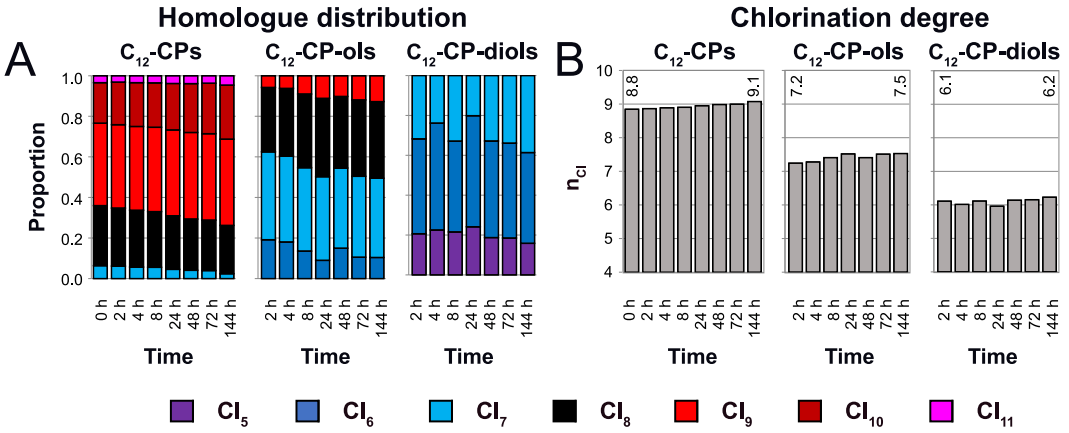

Fig. 4. Changes of homologue distributions (A) and chlorination degrees (B) and of non-, mono- and di-hydroxylated chloroparaffins. Exposure of chlorinated dodecanes with the dehalogenase LinB up to 144 h resulted in the formation of mono- and di-hydroxylated products. Nona- (red) and octa- (black) chlorinated homologues are most abundant in the C_{12}-CP fraction. Octa- (black) and hepta- (light blue) chlorinated homologues dominate in C_{12}-CP-ol fractions, while hepta- (light blue) and hexa- (blue) chlorinated materials are most abundant in C_{12}-CP-diol fractions. (For interpretation of the references to colour in this figure legend, the reader is referred to the Web version of this article.)

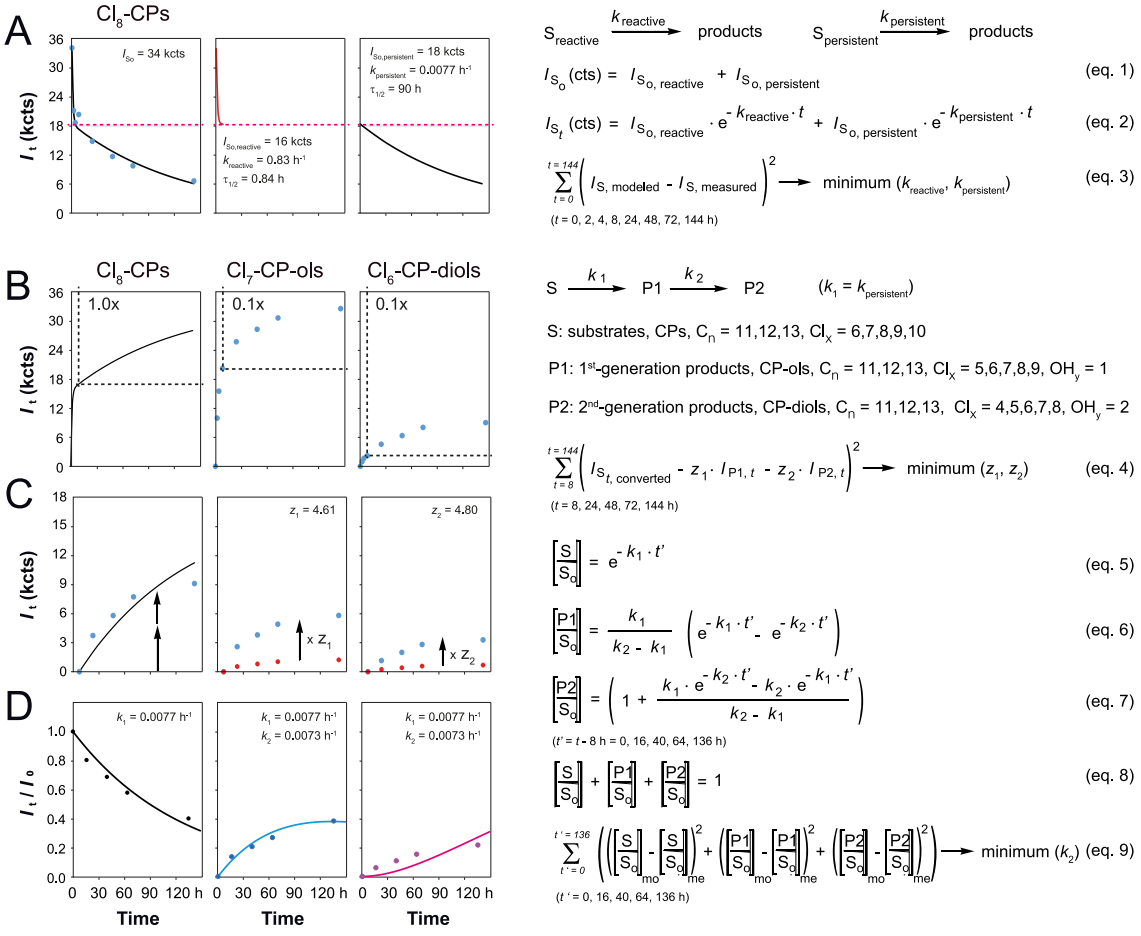

Fig. 5. Kinetic models, response factor corrections and equations for the LinB-catalyzed dehalohydroxylation of CPs. As an example, the stepwise conversion of Cl_8-CPs (substrate, S) to Cl_7-CP-ols (P1, first-generation product) and Cl_6-CP-diols (P2, second-generation product) is displayed. The LinB-catalyzed conversion of octa-chlorododecanes (A) can be split in a fast and slow reaction, in which reactive and persistent materials are converted, respectively (eqs. 1-3, Knobloch et al., 2021b). MS response factors z_1 and z_2 for mono- and di-hydroxylated products are deduced from eq. 4 (B, C). A kinetic model, describing the conversion of persistent CP-material (t' = t - 8 h) and the formation of first- (blue) and second- (magenta) generation products (P1, P2), is deduced from response factor-corrected data (D) and from eqs. 5-9. Modeled first-order rate constants k_1 and k_2 are indicated. (For interpretation of the references to colour in this figure legend, the reader is referred to the Web version of this article.)

3.5. Kinetic models for LinB-catalyzed dechlorination and hydroxylation reactions

A first kinetic model describing the LinB-catalyzed transformation of CPs and COs was introduced before (Knobloch et al., 2021b). In this study, a more elaborate kinetic model that includes the conversion of starting material and the formation of first- and second-generation products was established. This model enables estimating CP-, CP-ol- and CP-diol-proportions during biosynthesis with LinB. The model is explained in Fig. 5 on the example of octa-chlorododecanes ($C_{12}Cl_8$-CPs).

Fig. 5A displays trends of non-interfered $I_{100\%}$ signals (cts) of octa-chlorododecanes after 0, 2, 4, 8, 24, 48, 72 and 144 h LinB exposure. A quick drop of the signal intensity from 34 kcts to about 18 kcts was observed in the first 8 h. Conversion of the remaining material is much slower in a second phase and not complete, even after one week of exposure. We introduced a model for this two-phase kinetics (Knobloch et al., 2021b) and reported that each CP homologue class contains both, reactive ($I_{S0,\ reactive}$) and more persistent ($I_{S0,\ persistent}$) material (Fig. 5 eq. 1). A two-phase kinetic model (eq. 2) with first-order rate constants $k_{reactive}$ and $k_{persistent}$ can describe these trends. Estimates for $k_{reactive}$ and $k_{persistent}$ were obtained through minimization (eq. 3). They are listed in Table S31. A similar approach has been used before to model transformations of chloroparaffins to chloroolefins by the dehydrohalogenase LinA (Heeb et al., 2019). First-order rate constants of reactive and persistent materials differ up to two orders of magnitude (Table S31). In other words, reactive CPs, which are transformed with half-lifes $\tau_{1/2} < 1$ h, are converted completely within the first 8 h (Fig. 5A). Only the conversion of more persistent material with half-lifes $\tau_{1/2} \approx 100$ h, can be studied after 8 h of exposure.

In the following, we developed more elaborate kinetic models to describe the stepwise dehalohydroxylation of persistent CPs (S) to respective CP-ols and CP-diols (Fig. 5B). First-order rate constants k_1 and k_2 describe the uni-directional conversion of CP substrates to first- (P1) and second- (P2) generation products with lower chlorination and higher hydroxylation degrees.

Fig. 5B displays the formation of hepta-chloroparaffin-ols (Cl_7-CP-ols, cyan) and hexa-chloroparaffin-diols (Cl_6-CP-diols, magenta). Signal intensities ($I_{100\%}$, cts) of the mono- and dihydroxylated products are considerably lower (~0.1x) than those of CPs and do not add up to the signal intensities of converted CP-material. This is due to lower MS-response of the formed products.

Mass spectrometric evidence was presented that CPs, CP-ols and CP-diols all form chloride-adduct ions $[M+Cl]^-$ under the given CE-APCI conditions (Knobloch et al., 2021a). It has been shown, that the MS response of CPs depends on the chlorination degree and lower-chlorinated homologues show lower responses (Mézière et al., 2020). Therefore, it can be expected that dehalohydroxylation products show lower MS responses too. To compensate for this, relative response factors z_1 and z_2 for CP-ols and CP-diols were deduced by minimizing the difference of the converted signal and the newly formed signal (Fig. 5C, eq. 4). In other words, response factors were modeled based on the assumption that the signal intensities of formed CP-ols and CP-diols are equal to the signal intensity of converted CPs. In this and other studies, no evidence could be found that LinB transforms CPs to other transformation products than dehalohydroxylated ones (Knobloch et al., 2021a, 2021b). According to eq. 4, differences of the signal intensities of converted substrates ($I_{S,\ converted}$, cts) and of response factor-corrected CP-ols (I_{P1}, cts) and CP-diols (I_{P2}, cts) were minimized. For the conversion of Cl_8-CPs to Cl_7-CP-ols and Cl_6-CP-diols, relative response factors $z_1 = 4.61$ and $z_2 = 4.80$ were obtained. Table S32 lists relative response factors for all CP-ols and –diols studied. They vary from 2.32 to 11.74.

With this, the kinetics of the substrate conversion in relation to the initial concentration of persistent material $[S/S_o]$ was described with the exponential function eq. 5 (Fig. 5). According to eq. 6 and eq. 7, the formation of first- and second-generation products were modeled. Squared differences of modeled and measured intensities for substrates $[S/S_o]$, first- $[P1/S_o]$ and second- $[P2/S_o]$ generation products were minimized (eq. 9), resulting in estimates for k_2. Estimates for k_1, which correspond to $k_{persistent}$, are robust and were not minimized again (Fig. 5D).

3.6. Homologue-specific kinetic models for the stepwise dehalohydroxylation of SCCPs

Fig. 6 displays the modeled kinetics of hepta- to deca-chlorinated C_{11}-, C_{12}- and C_{13}-homologues, together with the measured data of C_{12}-homologues. Measured C_{11}- and C_{13}-data is shown in Fig. S8. The stepwise conversion of hepta-chlorododecanes (Cl_7-CPs, black) to hexa-chlorododecanols (Cl_6-CP-ols, blue) and penta-chloro-dodecan-diols (Cl_5-CP-diols, magenta) as first- and second-generation products is shown in Fig. 6A (upper left diagram). Accordingly, octa- (Cl_8), nona- (Cl_9) and deca- (Cl_{10}) chloro-undecanes, -dodecans and -tridecans (black) are converted by LinB to respective mono- (blue) and di- (magenta) hydroxylated products (Fig. 6B).

As mentioned, these homologue-specific kinetic models describe the conversion of more persistent CPs, the formation and accumulation of CP-ols and their transformation to CP-diols according to equations 6, 7 and 8 (Fig. 5). Measured data points are affected by low signal-to-noise ratios, especially the ones of CP-ols and CP-diols. Despite some scatter in the data, systematic trends were observed, best seen from overlaid diagrams (Fig. 6). These diagrams indicate that the chlorination degree (Fig. 6 right) is more influential with respect to conversion rates than the carbon chain length (Fig. 6, B). For example, rate constants k_1 decreased gradually from 0.0120 to 0.0077, 0.0066 and 0.0053 h^{-1} for Cl_7-, Cl_8-, Cl_9- and Cl_{10}-chloro-dodecanes (Fig. 6A). Similar trends were observed for chloro-undecanes and -tridecanes (Fig. S8). Table S32 lists first-order rate constants (k_1, k_2) and respective half-lifes ($\tau_{1/2}$). Effects of carbon-chain length on k_1 were smaller and changed e.g. for Cl_8-chloro-undecanes, -dodecanes and -tridecanes from 0.0066 to 0.0077 to 0.0083 h^{-1}.

In general, the conversion of CPs (black) and the formation of CP-diols (magenta) can be described well with the modeled rate constants k_1 and k_2, while the scatter in the CP-ol data (blue) is larger (Fig. 6). Relevant amounts of CP-diols (magenta) accumulated with time, especially when exposing lower-chlorinated substrates to LinB. In most cases, k_2 was larger than k_1, explaining why CP-ols only accumulate to some degree in an early phase and are converted further to CP-diols in a later phase. In other words, lower-chlorinated CP-ols are more reactive than their parent CPs ($k_2 > k_1$). k_2 decreased as well with chlorination degree. For example, k_2 for the transformation of Cl_6-, Cl_7-, Cl_8- and Cl_9-chlorododecan-ols to respective -diols decreases from 0.017 to 0.0073, 0.0061 and 0.0020 h^{-1}. Respective k_2/k_1 ratios change from 1.4, 0.9, 0.9 to 0.4 explaining why lower-chlorinated CP-ols did hardly accumulate during long exposure.

Fig. 7A displays mean proportions of CPs (black), CP-ols (blue) and CP-diols (magenta) of different homologues during LinB exposure for 0, 16, 40, 64 and 136 h (t' = t – 8 h). Table S33 lists individual data for C_{11}-, C_{12}- and C_{13}-homologues together with corresponding hydroxylation degrees (n_{OH}). Only a moderate influence of the carbon-chain length has been observed on n_{OH} (Table S33). Fig. 7B represents mean n_{OH} values with standard deviations.

A gradual decrease of CP proportions (black) during LinB exposure is observed in all cases. After 136 h, mean CP proportions of 16 ± 0% 25 ± 2%, 39 ± 1%, 45 ± 2% and 53 ± 1% were observed for Cl_6-, Cl_7-, Cl_8-, Cl_9- and Cl_{10}-CPs, respectively (Fig. 7A). Respective CP-diol proportions (magenta) after 136 h decreased from 84 ± 0% to 55 ± 6%, 34 ± 9%, 24 ± 6% and 13 ± 7%. Lower-chlorinated CP-ols (blue) are quickly formed and accumulate to some degree (<40 h), but are converted completely in the later phase. However, higher-chlorinated CP-ols could still be detected after 136 h exposure. Respective proportions were 0 ± 0%, 20 ± 8%, 27 ± 8%, 31 ± 6% and 34 ± 9% (Fig. 7A).

Fig. 7B displays mean (n = 3) hydroxylation degrees (n_{OH}), which

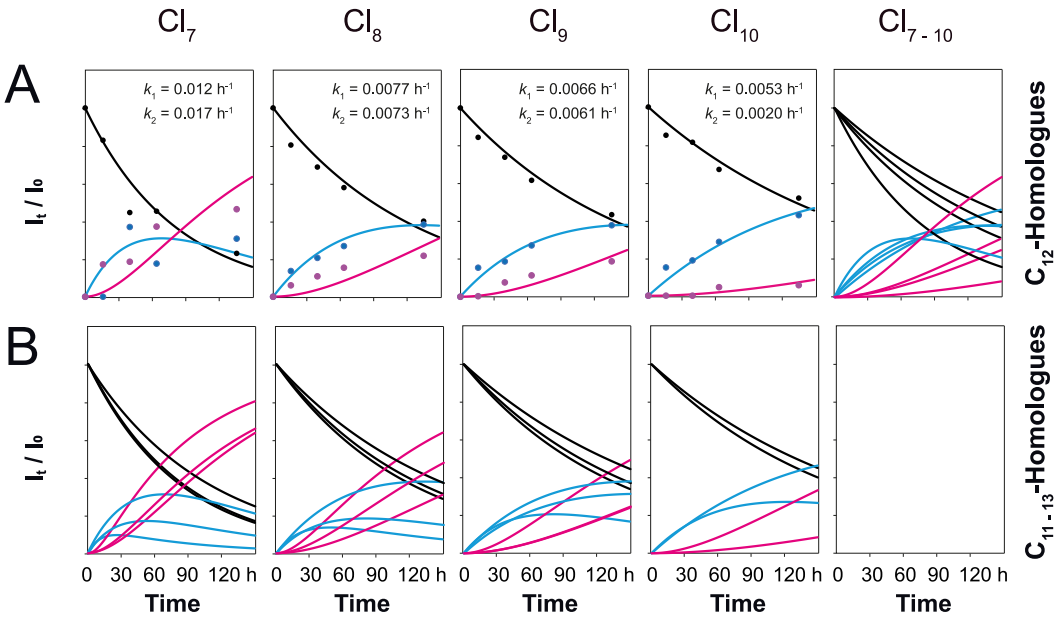

Fig. 6. Homologue-specific kinetic models for a stepwise dehalohydroxylation of persistent CPs by LinB. Different CP homologues (substrates, S, black) are transformed to CP-ols (first-generation products, P1, blue) and CP-diols (second-generation products, P2, magenta). The chlorination degree of the CP starting material is indicated (top). Measured (dots) and modeled (lines) C_{12}-data are shown (A), the ones of C_{11}- and C_{13}-homologues are shown in Figure S8. Modeled kinetics of C_{11}-, C_{12}-, and C_{13}-homologues are compared (B). First-order rate constants for the formation of C_{12}-CP-ols (k_1) and C_{12}-CP-diols (k_2) are indicated. A strong dependence of the chlorination degree (right diagram), but only moderate effects of the carbon chain length (lower diagrams) are noticed for the conversion kinetics of different SCCP homologues. (For interpretation of the references to colour in this figure legend, the reader is referred to the Web version of this article.)

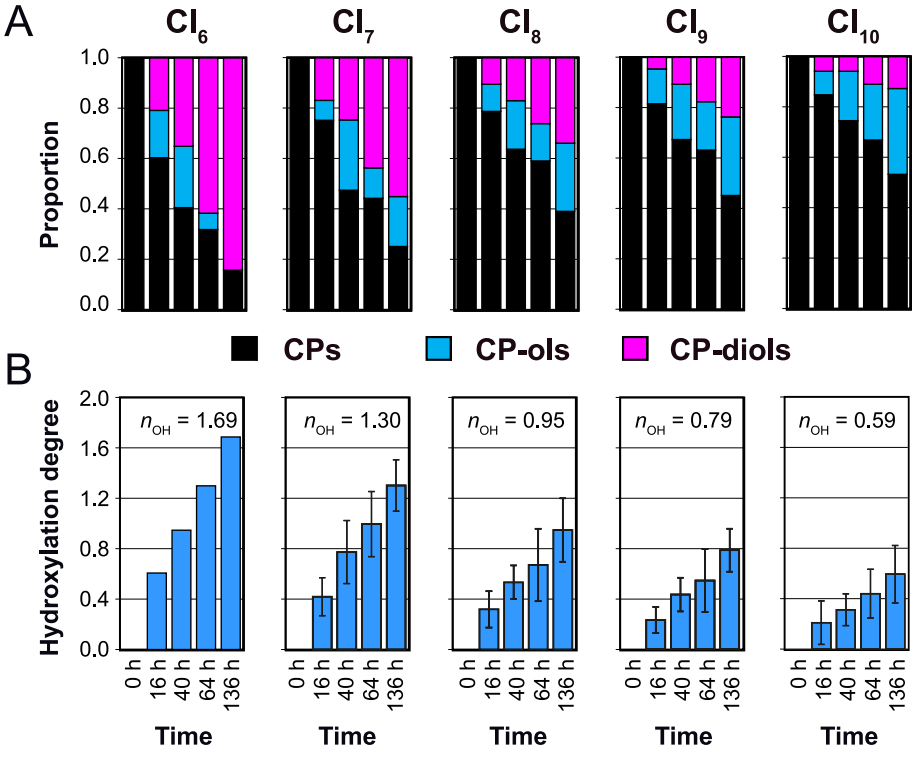

Fig. 7. Distribution of CPs and their transformation products (A) and respective hydroxylation degrees ($n_{OH,}$ B) during LinB-exposure. Mean pattern of CPs (black), CP-ols (blue) and CP-diols (magenta) are compared, as found in exposed chloro-undecanes, -dodecanes and –tridecanes. Exposure times (t') of 0, 16, 40, 64 and 136 h refer to LinB exposure after reaching the slower second phase. During CP-ol and CP-diol formation, respective hydroxylation degrees increase with time, most pronounced when starting with lower-chlorinated CP-homologues (Cl_6). (For interpretation of the references to colour in this figure legend, the reader is referred to the Web version of this article.)

increased during LinB exposure in all cases. Data for individual homologue families are listed in Table S33. After 136 h, mean n_{OH} values of 1.69 ± 0.00, 1.30 ± 0.20, 0.95 ± 0.25, 0.79 ± 0.17 and 0.59 ± 0.23 were obtained. This also indicates that the hydroxylation of lower-chlorinated CPs is preferential, while levels of hydroxylated products are lower when starting with higher-chlorinated materials (Fig. 7B).

4. Conclusions

The stepwise hydrolysis of CPs catalyzed by LinB leads to diverse mixtures of hydroxylated CPs. The qualitative as well as the quantitative analysis of such complex mixtures is challenging. The lack of analytical standards further complicates the issue (Schinkel et al., 2018a; Fernandes et al., 2022). In 2017, short-chain CPs (C_{10}- to C_{13}-CPs) have

been included in the Stockholm Convention POP list (UNEP, 2017b). Technical SCCPs are already mixtures of hundred thousands of constitutional isomers and stereoisomers. Thus, any hydroxylation reaction leads to mixtures of probably millions of different products.

In this study, we synthesized 30 new classes of mono- and di-hydroxy CPs with the bacterial enzyme LinB. Only little is known about these CP-transformation products. The provided chromatographic and mass spectrometric data is helpful to identify such substances. Furthermore, the LinB-catalyzed synthesis can be used to produce larger amounts of hydroxylated CP-materials, useful as analytical reference material and starting materials for toxicological and environmental fate studies.

The transformation of CPs with LinB revealed that each homologue class contains both, reactive and more persistent material. Depending on the chlorination degree, 32–82% of the exposed CPs are reactive and converted quickly by LinB (<8 h). As consequence, 18–68% of the material can be classified as more persistent against LinB. While reactive CPs were converted within hours ($\tau_{1/2}$ = 0.5–3.2 h), more persistent material was transformed about 100-times slower, within several days only ($\tau_{1/2}$ = 56–162 h).

LinA, another dehalogenase expressed by *Sphingobium indicum* bacteria, converts SCCPs to chloroolefins (Heeb et al., 2019). The LinA-transformation study also revealed that both, reactive ($\tau_{1/2}$ = 1.7–5.8 h) and persistent material ($\tau_{1/2}$ = 150–250 h) is present in CP-mixture. Thus, we conclude that both enzymes, which were exposed to thousands of CP isomers, were selective. More reactive isomers were converted quickly, more persistent ones accumulated in relative amounts.

The chlorination degree of CPs was found to be more influential on conversion rates and persistency than the carbon-chain length. Lower-chlorinated homologues are more reactive with respect to LinB, while higher-chlorinated material is converted preferentially by LinA (Heeb et al., 2019). LinA and LinB, both catalyze the cleavage of carbon-halogen bonds. Therefore, it is plausible that the halogenation degree is more relevant for this chemistry than the carbon-chain length. This may be different for other enzymes e.g. monooxygenases which break carbon-hydrogen bonds (Fig. 1E).

Interactions of CPs with both enzymes are possibly selective too, as it is observed for HCHs (Raina et al., 2007) and HBCDs (Heeb et al., 2018). Some isomers are converted quickly, while others accumulate in the remaining material. We assume that interactions of complex CP-mixtures with other enzymes are selective too. Therefore, we expect that technical CP-mixtures, in general contain both, reactive and persistent material. Rates for enzymatic transformations may vary orders of magnitude, even for isomers of the same homologue class.

Current legislation has banned SCCPs and with it induced a shift to use medium- and long-chain CPs instead. With respect to the persistence of SCCPs, we found that the chlorination degree of the material is more relevant than the carbon-chain length, at least for the *in-vitro* transformation with the LinA and LinB enzymes. It is not clear yet if the chlorination degree is also more important for the bioaccumulation potential and toxicity of CPs than the carbon-chain length. These questions should be answered in the risk assessment for longer-chain CPs.

Credit author statement

Marco Knobloch: Methodology, Validation, Software, Data curation, Supervision, Formal analysis, Investigation, Visualization, Writing – original draft, Review & Editing. Flurin Mathis: Methodology, Investigation, Data curation, Software, Formal analysis, Visualization, Review & Editing. Thomas Fleischmann: Methodology, Validation, Investigation, Review & Editing. Hans-Peter Kohler: Conceptualization, Resources, Supervision, Review & Editing. Susanne Kern: Supervision, Project administration, Resources, Methodology, Review & Editing. Davide Bleiner: Supervision, Project administration, Review & Editing. Norbert Heeb: Conceptualization, Methodology, Validation, Project administration, Funding acquisition, Resources, Supervision, Software, Formal analysis, Visualization, Writing – original draft, Review & Editing.

Declaration of competing interest

The authors declare that they have no known competing financial interests or personal relationships that could have appeared to influence the work reported in this paper.

Acknowledgement

This work was supported by the Swiss Federal Office for the Environment (BAFU) (grant number: 19.0011.PJ/S113-1600).

Appendix A. Supplementary data

Supplementary data to this article can be found online at https://doi.org/10.1016/j.chemosphere.2021.132939.

References

Belkin, S., 1992. Biodegradation of haloalkanes. Biodegradation 3, 299–313. https://doi.org/10.1007/BF00129090.

Bogdal, C., Alsberg, T., Diefenbacher, P.S., Macleod, M., Berger, U., 2015. Fast quantification of chlorinated paraffins in environmental samples by direct injection high-resolution mass spectrometry with pattern deconvolution. Anal. Chem. 87, 2852–2860. https://doi.org/10.1021/ac504444d.

Chen, W., Yu, M., Zhang, Q., Hou, X., Kong, W., Wei, L., Mao, X., Liu, J., Schnoor, J.L., Jiang, G., 2020. Metabolism of SCCPs and MCCPs in suspension rice cells based on paired mass distance (PMD) analysis. Environ. Sci. Technol. 54, 9990–9999. https://doi.org/10.1021/acs.est.0c01830.

Faber, K., 2018. Biotransformations in Organic Chemistry, Trends in Biotechnology. Springer International Publishing, Cham. https://doi.org/10.1007/978-3-319-61590-5.

Fernandes, A.R., Vetter, W., Dirks, C., van Mourik, L., Cariou, R., Sprengel, J., Heeb, N., Lentjes, A., Krätschmer, K., 2022. Determination of chlorinated paraffins (CPs): analytical conundrums and the pressing need for reliable and relevant standards. Chemosphere 286. https://doi.org/10.1016/j.chemosphere.2021.131878.

Fiedler, H., 2010. Short-chain chlorinated paraffins: production, use and international regulations. In: The Handbook of Environmental Chemistry - Chlorinated Paraffins. Springer Nature, pp. 1–40. https://doi.org/10.1007/698.

Glüge, J., Wang, Z., Bogdal, C., Scheringer, M., Hungerbühler, K., 2016. Global production, use, and emission volumes of short-chain chlorinated paraffins – a minimum scenario. Sci. Total Environ. 573, 1132–1146. https://doi.org/10.1016/j.scitotenv.2016.08.105.

He, C., van Mourik, L., Tang, S., Thai, P., Wang, X., Brandsma, S.H., Leonards, P.E.G., Thomas, K.V., Mueller, J.F., 2020. In vitro biotransformation and evaluation of potential transformation products of chlorinated paraffins by high resolution accurate mass spectrometry. J. Hazard. Mater. 124245 https://doi.org/10.1016/j.jhazmat.2020.124245.

Heeb, N.V., Zindel, D., Geueke, B., Kohler, H.P.E., Lienemann, P., 2012. Biotransformation of hexabromocyclododecanes (HBCDs) with LinB - an HCH-converting bacterial enzyme. Environ. Sci. Technol. 46, 6566–6574. https://doi.org/10.1021/es2046487.

Heeb, N.V., Zindel, D., Graf, H., Azara, V., Bernd Schweizer, W., Geueke, B., Kohler, H.-P. E., Lienemann, P., 2013. Stereochemistry of LinB-catalyzed biotransformation of δ-HBCD to 1R,2R,5S,6R,9R,10S-pentabromocyclododecanol. Chemosphere 90, 1911–1919. https://doi.org/10.1016/j.chemosphere.2012.10.019.

Heeb, N.V., Mazenauer, M., Wyss, S., Geueke, B., Kohler, H.P.E., Lienemann, P., 2018. Kinetics and stereochemistry of LinB-catalyzed Δ-HBCD transformation: comparison of in vitro and in silico results. Chemosphere 207, 118–129. https://doi.org/10.1016/j.chemosphere.2018.05.057.

Heeb, N.V., Schalles, S., Lehner, S., Schinkel, L., Schilling, I., Lienemann, P., Bogdal, C., Kohler, H.P.E., 2019. Biotransformation of short-chain chlorinated paraffins (SCCPs) with LinA2: a HCH and HBCD converting bacterial dehydrohalogenase. Chemosphere 226, 744–754. https://doi.org/10.1016/j.chemosphere.2019.03.169.

Heeb, N.V., Iten, S., Schinkel, L., Knobloch, M., Sprengel, J., Lienemann, P., Bleiner, D., Vetter, W., 2020. Characterization of synthetic single-chain CP standard materials – removal of interfering side products. Chemosphere 255, 126959. https://doi.org/10.1016/j.chemosphere.2020.126959.

Knobloch, M.C., Schinkel, L., Schilling, I., Kohler, H.-P.E., Lienemann, P., Bleiner, D., Heeb, N.V., 2021a. Transformation of short-chain chlorinated paraffins by the bacterial haloalkane dehalogenase LinB – formation of mono- and di-hydroxylated metabolites. Chemosphere 262, 128288. https://doi.org/10.1016/j.chemosphere.2020.128288.

Knobloch, M.C., Schinkel, L., Kohler, H.-P.E., Mathis, F., Kern, S., Bleiner, D., Heeb, N.V., 2021b. Transformation of short-chain chlorinated paraffins and olefins with the bacterial dehalogenase LinB from Sphingobium Indicum – kinetic models for the

homologue-specific conversion of reactive and persistent material. Chemosphere 283, 131199. https://doi.org/10.1016/j.chemosphere.2021.131199.

Lal, R., Pandey, G., Sharma, P., Kumari, K., Malhotra, S., Pandey, R., Raina, V., Kohler, H.-P.E., Holliger, C., Jackson, C., Oakeshott, J.G., 2010. Biochemistry of microbial degradation of hexachlorocyclohexane and prospects for bioremediation. Microbiol. Mol. Biol. Rev. 74, 58–80. https://doi.org/10.1128/MMBR.00029-09.

Li, C., Xie, H.-B., Chen, J., Yang, X., Zhang, Y., Qiao, X., 2014. Predicting gaseous reaction rates of short chain chlorinated paraffins with #OH: overcoming the difficulty in experimental determination. Environ. Sci. Technol. 48, 13808–13816. https://doi.org/10.1021/es504339r.

Li, Y., Hou, X., Chen, W., Liu, J., Zhou, Q., Schnoor, J.L., Jiang, G., 2019. Carbon chain decomposition of short chain chlorinated paraffins (SCCPs) mediated by pumpkin and soybean seedlings. Environ. Sci. Technol. 53, 6765–6772. https://doi.org/10.1021/acs.est.9b01215.

Mézière, M., Krätschmer, K., Pe Rkons, I., Zacs, D., Marchand, P., Dervilly, G., Le Bizec, B., Schächtele, A., Cariou, R., Vetter, W., 2020. Addressing main challenges regarding short- and medium-chain chlorinated paraffin analysis using GC/ECNI-MS and LC/ESI-MS methods. J. Am. Soc. Mass Spectrom. 31, 1885–1895. https://doi.org/10.1021/jasms.0c00155.

Nagata, Y., Nariya, T., Ohtomo, R., Fukuda, M., Yano, K., Takagi, M., 1993. Cloning and sequencing of a dehalogenase gene encoding an enzyme with hydrolase activity involved in the degradation of γ-hexachlorocyclohexane in Pseudomonas paucimobilis. J. Bacteriol. 175, 6403–6410. https://doi.org/10.1128/jb.175.20.6403-6410.1993.

Raina, V., Hauser, A., Buser, H.R., Rentsch, D., Sharma, P., Lal, R., Holliger, C., Poiger, T., Müller, M.D., Kohler, H.P.E., 2007. Hydroxylated metabolites of β- and δ-hexachlorocyclohexane: bacterial formation, stereochemical configuration, and occurrence in groundwater at a former production site. Environ. Sci. Technol. 41, 4291–4298. https://doi.org/10.1021/es062908g.

Raina, V., Rentsch, D., Geiger, T., Sharma, P., Buser, H.R., Holliger, C., Lal, R., Kohler, H. P.E., 2008. New metabolites in the degradation of α- and γ- hexachlorocyclohexane (HCH): pentachlorocyclohexenes are hydroxylated to cyclohexenols and cyclohexenediols by the haloalkane dehalogenase LinB from Sphingobium indicum B90A. J. Agric. Food Chem. 56, 6594–6603. https://doi.org/10.1021/jf800465q.

Schinkel, L., Lehner, S., Heeb, N.V., Lienemann, P., McNeill, K., Bogdal, C., 2017. Deconvolution of mass spectral interferences of chlorinated alkanes and their thermal degradation products: chlorinated alkenes. Anal. Chem. 89, 5923–5931. https://doi.org/10.1021/acs.analchem.7b00331.

Schinkel, L., Bogdal, C., Canonica, E., Cariou, R., Bleiner, D., McNeill, K., Heeb, N.V., 2018a. Analysis of medium-chain and long-chain chlorinated paraffins: the urgent need for more specific analytical standards. Environ. Sci. Technol. Lett. 5, 708–717. https://doi.org/10.1021/acs.estlett.8b00537.

Schinkel, L., Lehner, S., Knobloch, M., Lienemann, P., Bogdal, C., McNeill, K., Heeb, N.V., 2018b. Transformation of chlorinated paraffins to olefins during metal work and thermal exposure – deconvolution of mass spectra and kinetics. Chemosphere 194, 803–811. https://doi.org/10.1016/j.chemosphere.2017.11.168.

Schinkel, L., Lehner, S., Heeb, N.V., Marchand, P., Cariou, R., McNeill, K., Bogdal, C., 2018c. Dealing with strong mass interferences of chlorinated paraffins and their transformation products: an analytical guide. TrAC Trends Anal. Chem. (Reference Ed.) 106, 116–124. https://doi.org/10.1016/j.trac.2018.07.002.

UNEP, 2016. Report of the Persistent Organic Pollutants Review Committee on the Work of its Twelfth Meeting. UNEP/POPS/POPRC.12/11/Add.3 1–36.

UNEP, 2017a. Decision SC-8/11 : Listing of Short-Chain Chlorinated Paraffins 14.

UNEP, 2017b. Additional Information Related to the Draft Risk Management Evaluation on Short-Chain Chlorinated Paraffins UNEP/POPS/POPRC.12/INF/7.

van Mourik, L.M., Gaus, C., Leonards, P.E.G., de Boer, J., 2016. Chlorinated paraffins in the environment: a review on their production, fate, levels and trends between 2010 and 2015. Chemosphere 155, 415–428. https://doi.org/10.1016/j.chemosphere.2016.04.037.

Vogel, T.M., Criddle, C.S., McCarty, P.L., Arcos, J.C., 1987. Transformations of halogenated aliphatic compounds: oxidation, reduction, substitution, and dehydrohalogenation reactions occur abiotically or in microbial and mammalian systems. Environ. Sci. Technol. 21, 722–736. https://doi.org/10.1021/es00162a001.